Structure and electron correlation of Mn on Ni(110)

O. Rader,* T. Mizokawa,† and A. Fujimori
Department of Physics, University of Tokyo, 7-3-1 Hongo, Bunkyo-ku, Tokyo 113-0033, Japan

A. Kimura
Department of Physical Sciences, Graduate School of Science, Hiroshima University, 1-3-1 Kagamiyama, Higashi-Hiroshima 739-8526, Japan

(Received 23 May 2001; published 8 October 2001)

We have deposited Mn on the (110) surface of Ni and discover ordering into a $c(2\times2)$ superstructure for coverages of 0.35–0.5 monolayer Mn. Mn $2p$ photoemission spectra show distinct satellite structures which disappear for higher Mn coverage. Calculations using configuration-interaction theory including multiplet effects on a model cluster representing the local geometry of a surface alloy identify the features as correlation satellites and give model parameters as follows: charge-transfer energy $\Delta=1$ eV, Coulomb energy $U=3$ eV, and transfer integral $T=1.2$ eV. A detailed comparison to the case of $c(2\times2)$ Mn/Cu(100) leads to the conclusion that $c(2\times2)$ Mn/Ni(110) is a new magnetic surface alloy.

DOI: 10.1103/PhysRevB.64.165414 PACS number(s): 79.60.Dp, 73.20.Hb

I. INTRODUCTION

A new material class termed *ordered magnetic surface alloys* has recently been characterized by Wuttig, Gauthier, and Blügel.[1,2] Materials pertaining to this class consist of a metallic crystal surface on top of which atoms that bear a magnetic moment arrange in a certain superstructure. This structure differs not only laterally from a simple $p(1\times1)$-type overlayer: Experimental and theoretical structure determinations revealed that the adsorbate occupies sites of the surface atomic layer of the substrate, however at a comparatively large outward relaxation. For the first ordered magnetic surface alloy that has fully been characterized, the system $c(2\times2)$ Mn/Cu(100) formed by deposition of the mass equivalent of 0.5 monolayer (ML) Mn, this outward relaxation amounts to 14% of the Cu(100) interlayer distance.[1] Subsequent to the characterization of this system, another manganese surface alloy has been identified: $c(2\times2)$ Mn/Ni(100).[3] In addition to these surface alloys at nominal half-monolayer Mn coverage, more complicated structures have been identified for deposited amounts beyond 0.5 ML like the $p2mg(4\times2)$ Mn/Cu(100) structure.[4] The stability of these systems has been studied by *ab initio* total-energy calculations with the result that they are stabilized by the presence of the magnetic moment; i.e., the structures would not form for a paramagnetic Mn atom.[1,2]

Interesting magnetic properties have been predicted. The Mn-Mn distance in the $c(2\times2)$ Mn/Cu(100) system is by a factor of $\sqrt{2}$ larger than in bulk fcc metals like Cu. This increased distance is expected to revert the magnetic coupling between Mn moments from antiparallel to parallel causing long-range ferromagnetic order.[1] Experimentally, however, neither magnetic circular x-ray dichroism at room temperature[5] nor spin-resolved photoemission at liquid-nitrogen temperature[6] have yet been able to confirm this interesting prediction for $c(2\times2)$ Mn/Cu(100). On the other hand, the surface-alloy system $c(2\times2)$ Mn/Ni(100) orders ferromagnetically with parallel coupling of the Mn moments to the magnetization of the Ni substrate as seen from magnetic circular x-ray dichroism measurements.[5,7] Temperature-dependent studies show that ferromagnetic order is caused by the ferromagnetism of the Ni substrate and that the Mn follows the magnetization of the Ni surface atomic layer.[7]

In a complete study of the occupied and unoccupied electronic structure of $c(2\times2)$ Mn on Cu(100) it has been observed that the exchange splitting of Mn $3d$ is almost twice as large in photoemission and inverse photoemission than from first-principles calculations.[6] For $c(2\times2)$ Mn/Ni(100) the experimental value exceeds the theoretical one still by a factor of 1.5.[6] In addition, the angle dispersion of Mn $3d$ minority-spin states has been found to be very small (110 meV) for $c(2\times2)$ Mn/Cu(100).[6] Both observations indicate strong correlation of $3d$ electrons in the $c(2\times2)$ structure. This has been verified by the observation of a valence-band satellite structure for $c(2\times2)$ Mn/Cu(100) with prominent peaks at 8 eV and 9.6 eV binding energy.[8] In order to distinguish the Mn-derived valence-band satellite from the well-known Cu-derived satellite peaks at 11.8 eV and 14.6 eV, the assignment of the Mn-derived satellite has been done on the basis of resonant photoemission at the Mn $3p$ excitation threshold. Interestingly, Mn $2p$ core-level photoemission spectra also show intense satellite structures for $c(2\times2)$ Mn/Cu(100), and this fact renders identification of correlation effects in an element-selective manner particularly convenient.[8] For this system, the positions of Mn $3d$ states in photoemission and inverse photoemission, of the valence-band satellite, and of the Mn $2p$ core-level satellite have been used in Ref. 8 to consistently describe the system with a simple configuration-interaction cluster model and to derive model parameters.

It is interesting to ask whether the class of ordered magnetic surface alloys is limited to Mn on (100) surfaces of Cu and Ni or whether further members can be identified. In fact, 0.5 ML $c(2\times2)$ Mn/Cu(110) has been characterized as surface alloy.[9] On the other hand, the $c(2\times2)$ superstructure of Mn/Ag(100) has been identified as a double-layer surface alloy involving 1.5 ML Mn.[10] On fcc Co(100), Mn has been found to grow as $p(1\times1)$ overlayer;[11] however, weak $c(2\times2)$ low-energy electron diffraction (LEED) spots

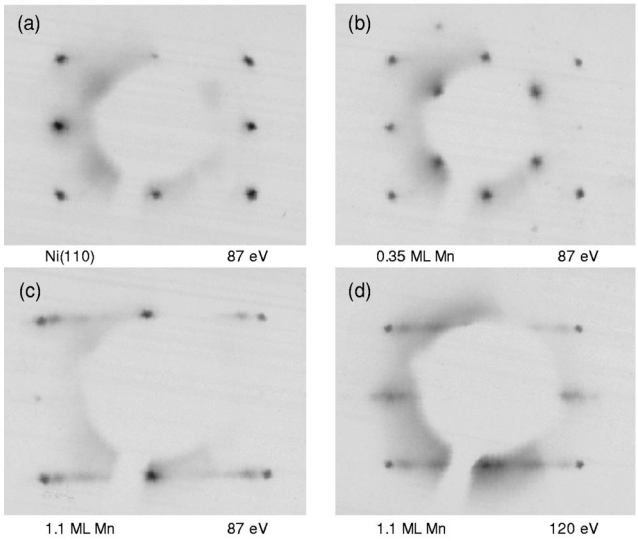

FIG. 1. LEED patterns of (a) clean Ni (110) and (b) 0.35 ML $c(2\times2)$ Mn/Ni(110) taken at 87 eV and of 1.1 ML (7×1) Mn/Ni(110) taken at 87 eV (c) and at 120 eV (d). (c) is a closeup.

have recently been reported for 0.3–0.8 ML coverage and considered as indication for surface alloy formation.[12] On Fe(100) and Fe(110), on the other hand, only $p(1\times1)$ Mn superstructures have been observed and interpreted as layer growth without interdiffusion.[13,14] Interestingly, a weak $c(2\times2)$ superstructure has also been found for 1 ML Co/Cu(100) after annealing.[15]

In the present work, Mn is deposited on Ni(110), and a $c(2\times2)$ structure appears around half-monolayer coverage. We study electron correlation effects on the electronic structure. Ni as substrate poses a similar problem to the assignment of valence-band features as the one mentioned above for Cu: countless satellite lines have been distinguished between 6 eV and 35 eV binding energy for pure Ni.[16] Therefore, we use Mn $2p$ x-ray photoelectron spectroscopy. We observe a distinct satellite which disappears together with the $c(2\times2)$ superstructure for higher Mn coverage. The satellite is similar to but weaker than the one observed for $c(2\times2)$ Mn/Cu(100) in agreement with the expectation of somewhat larger hybridization between Mn and Ni as compared to the case of Mn and Cu. We used the experience gained in previous analyses[8] of Mn-based surface alloys and analyze the spectra using a corresponding configuration-interaction cluster model.

II. EXPERIMENTS

Experiments were done in a vacuum chamber equipped with standard tools for surface preparation and characterization like LEED as well as a spherical electrostatic analyzer (VG CLAM) for x-ray photoelectron spectroscopy. We used Mg $K\alpha$ radiation for Mn $2p$ spectra. No correction for x-ray satellite lines has been done. Preparation of the Ni(110) single crystal has been performed *in situ* by Ne^+ ion bombardment and heating cycles until a sharp and intense $p(1\times1)$ LEED pattern was visible [Fig. 1(a)]. The

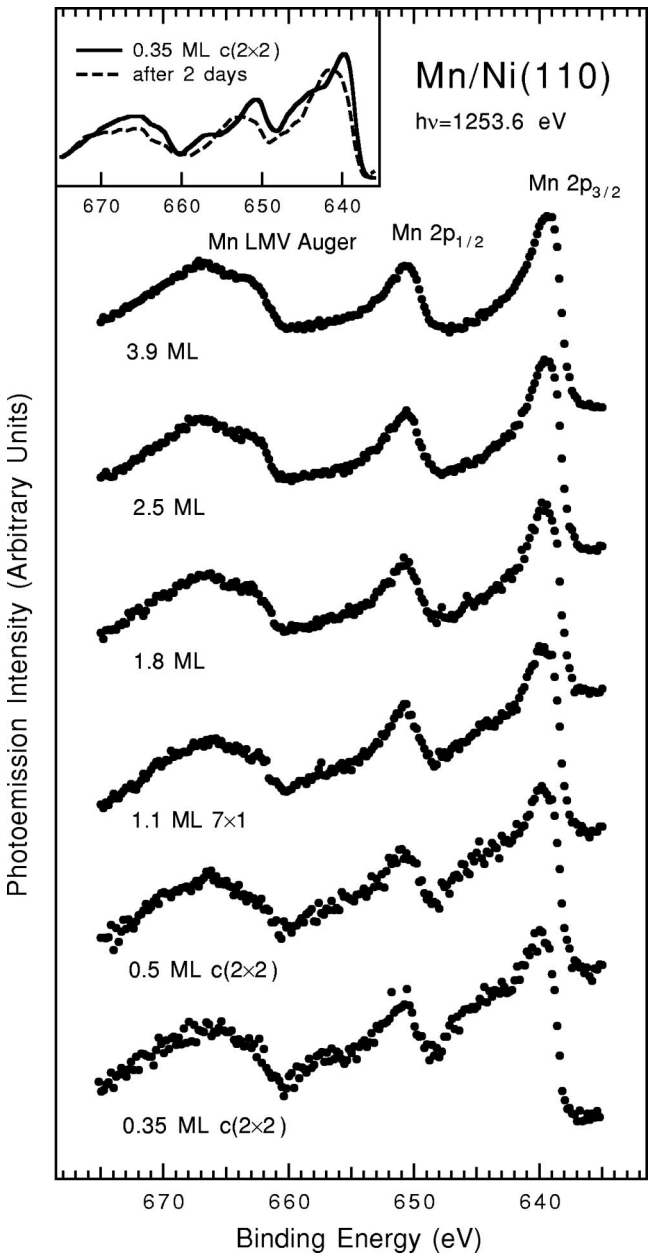

FIG. 2. Mn $2p$ core-level photoelectron spectra for various coverages of Mn on Ni(110). No background correction was done for all but the lowest two coverages, where a linear slope caused by the Ni substrate has been subtracted. Intense satellites about 5 eV below the main peaks appear in particular for the $c(2\times2)$ structure.

base pressure was in the upper 10^{-11} Torr range; e.g., when measuring the 0.35-ML spectrum shown in Fig. 2 the base pressure was 6.5×10^{-11} Torr and rose to 9.5×10^{-11} Torr during operation of the x-ray source. Mn has been evaporated from high-purity pieces by electron-beam heating enclosed in a water-cooled jacket. The deposition rate (0.7 ML/min) has been calibrated with an oscillating quartz and kept constant during *in situ* deposition by measuring the Mn ion current. This was particularly useful since spectra from different measurements had to be added. To keep sample contamination at a small level, we completed data aquisition for each sample in less than 2 h time, after which it was repre-

pared and the measurement reiterated. Moreover, we used a pass energy of 50 eV ensuring a high count rate. Spectra were taken with the sample at room temperature.

Figure 1(a) shows the $p(1\times1)$ LEED pattern of the clean Ni(110) substrate. For 0.35-ML [Fig. 1(b)] and 0.5-ML Mn coverage an intense $c(2\times2)$ superstructure is observed. The substrate temperature was kept at 70 °C during Mn deposition. This temperature has been found favorable for the growth of $c(2\times2)$ Mn on the (100) surface of Ni,[3] and in fact the present superstructure is as intense as the ones observed previously for $c(2\times2)$ Mn on (100) surfaces of Cu and Ni bulk crystals. Around the full monolayer coverage a 7×1 pattern is observed in Figs. 1(c) and 1(d). This structure could be a relaxed full Mn monolayer similar to the one obtained by deposition of 1 ML Mn on Cu(100) at low temperature ($<$270 K) which results in an 8×2 structure.[17] The thickest coverage deposited in the present work (3.9 ML) leads to a diffuse LEED pattern.

The Ni surface is reactive; this holds even more after Mn deposition. It should be noted in this context that oxygen does not generate a $c(2\times2)$ superstructure on Ni(110).[18] Rather, on the contrary, it has for Cu(110) been shown that the addition of oxygen destroys the Mn-induced $c(2\times2)$ superstructure.[9] The actual amount of contamination has in the present work been estimated from the ratio of O $1s$ versus Mn $2p_{3/2}$ photoemission intensities using tabulated sensitivity factors.[19] Clean surfaces are crucial in this experiment, and the sample with the lowest Mn coverage is most sensitive to a deterioration of the Mn $2p$ spectrum. For the lowest Mn coverage in Fig. 2 (0.35 ML), an oxygen coverage of not more than 0.05 ML results from our estimate. We have also measured the Mn $2p$ spectrum of a 0.35-ML-Mn sample after 2-day exposure to the residual gas and display it in the inset of Fig. 2. This spectrum shows that oxidization leads to a peak at a binding energy between the Mn main peak and the satellite peak (to be discussed below) of the Mn-induced $c(2\times2)$ structure. Moreover, the spectrum in the inset of Fig. 2 resembles the MnO_2 spectrum from Ref. 19.

Figure 2 shows the thickness dependence of Mn $2p$ core-level spectra. For the $c(2\times2)$ structure, we observe a broad and intense satellite about 5 eV below the $2p_{3/2}$ and $2p_{1/2}$ main peaks which has almost equal intensity for 0.35 and 0.5 ML. For 1.1 ML, the satellite already loses intensity, and for 1.8 ML the spectral shape approaches the one of bulk Mn metal without extra structures.

We will argue in the following section that the reduced Mn-Mn coordination in the $c(2\times2)$ structure, where ideally no Mn-Mn next-neighbor pairs exist, results in enhanced electron correlation giving rise to the satellite structures. This holds to a lesser extent also for the the 1.1-ML overlayer where Mn-Mn interaction is reduced due to the vacuum interface and due to missing subsurface Mn neighbors.

III. MODEL CALCULATIONS

For the $c(2\times2)$ structure, the Mn $2p$ excitation spectrum can be described by a simple configuration-interaction model on a Mn-Ni cluster. Previously, we have successfully employed a simpler model for the case of $c(2\times2)$ Mn/Cu(100).[8] In analogy to the cases of Mn on Cu(100), Cu(110), and Ni(100) we tentatively assign the behavior of LEED and photoemission to the formation of a surface alloy. As with these three similar surface alloys, which are structurally very similar to each other, a substantial outward relaxation can be expected. Interestingly, it has been argued that the intense superstructure LEED reflexes are not expected to occur for systems without such a substantial relaxation because of the proximity of the atomic numbers of Mn on the one hand and of Ni or Cu on the other hand.[2] We use for the present model the same Mn relaxation of $0.06a$ (where a is the substrate lattice constant) as obtained from the quantitative analysis for $c(2\times2)$ Mn/Cu(110), keeping in mind that the relaxations for $c(2\times2)$ Mn on Cu(100) and Ni(100) have been found to be very similar to each other.

The present data analysis method has widely been applied in studies on transition-metal compounds, and the reader may find basic aspects of the configuration-interaction cluster model in the review literature.[20] Core-level photoemission with its element sensitivity is particularly useful when combined with configuration-interaction calculations which include the multiplet effect and charge-transfer effect.[21–23] In particular, transition-metal $2p$ photoemission, which can efficiently be excited by conventional Mg and Al $K\alpha$ radiation, has been analyzed by configuration-interaction theory in a systematic way.[24,25] In the configuration-interaction calculation on the cluster-type model, while the multiplet effect is derived from the Coulomb interaction term between the transition-metal $2p$ core hole and transition-metal $3d$ electrons, the charge-transfer effect is due to the hybridization term between the transition-metal $3d$ orbitals and ligand orbitals. It has been found that the charge-transfer effect is more important than the multiplet effect to explain transition-metal $2p$ photoemission line shape observed in many transition-metal compounds.[24] (On the other hand, the multiplet effect is much more important than the charge-transfer one in transition-metal $2p$ x-ray absorption, x-ray emission, and electron-energy loss spectra.) Therefore, we used a version of the configuration-interaction cluster model in which the Coulomb interaction term is included in a simplified way[24] and, instead, the hybridization term between the Mn $3d$ and ligand orbitals in the Mn-Ni cluster is considered in an exact way.

Figure 3 shows the structural model used in the present work. It is more complex than the one used previously[8] due to the twofold symmetry of the fcc (110) surface. Two Ni atoms in the surface (S) layer (type 1, Mn-Ni distance $0.710a$ with a being the Ni lattice constant), four in the S-1 layer (type 2, $0.739a$), and one in the S-2 layer (type 3, $0.767a$) are considered; the two remaining atoms in the S layer are too far ($1.003a$) and therefore have been cut off. The ground state of the cluster considers three configurations, i.e.,

$$\psi_g = a_0|d^5\rangle + a_1|d^6\underline{L}\rangle + a_2|d^7\underline{L}^2\rangle.$$

Here, $\underline{L}$ denotes a ligand hole, which corresponds to the transfer of an electron from a Ni d orbital to a Mn d orbital.

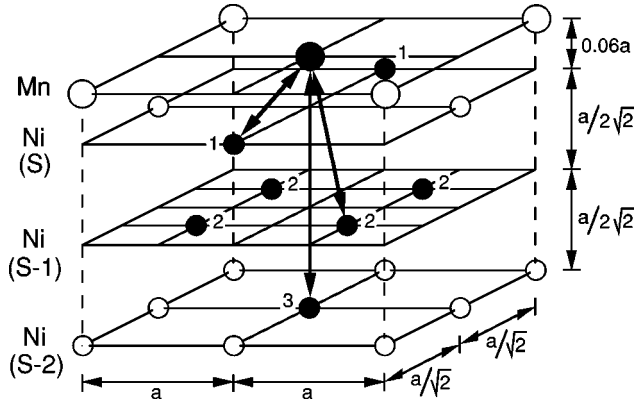

FIG. 3. Structural model employed in the configuration-interaction calculation for the $c(2\times2)$ superstructure. Positions of Mn (large circles) and Ni atoms (small circles). Hybridization between atoms marked by solid circles has been included in the model. For clarity, vertical distances appear expanded.

The energy associated with this charge transfer is $\Delta = E(d^6\underline{L}) - E(d^5)$. The Mn $3d$–Mn $3d$ Coulomb interaction energy is $U = E(d^6) + E(d^4) - 2E(d^5)$, where the energy $E(d^n\underline{L}^m)$ is the center of gravity of the multiplet corresponding to the $d^n\underline{L}^m$ configuration. The transfer integrals describing the hybridization between Mn $3d$ and Ni $3d$ are expressed in terms of Slater-Koster parameters $(dd\pi)$ and $(dd\sigma)$. Expressions for their anisotropy and distance dependence have been taken from Ref. 26. The final state of Mn $2p$ photoemission is given by

$$\psi_f = b_0|\underline{c}d^5\rangle + b_1|\underline{c}d^6\underline{L}\rangle + b_2|\underline{c}d^7\underline{L}^2\rangle,$$

where $\underline{c}$ represents a Mn $2p$ core hole. The Mn $2p$–Mn $3d$ Coulomb interaction energy Q has been tied to U by the typical assumption $U/Q = 0.8$. The Mn $2p$ photoemission intensity is given by

$$I_f \propto |a_0 b_0 + a_1 b_1 + a_2 b_2|^2$$

in the sudden approximation.

IV. ANALYSIS

The remaining parameters to be determined from the comparison to the experiment are Δ, U, and $T = (dd\sigma)$. Out of the two similar experimental spectra representing $c(2\times2)$ Mn, the 0.35-ML spectrum has been chosen for comparison to theory. The reason is that the Mn local geometry will not change if a few $c(2\times2)$ sites are left empty; however, excess Mn atoms will likely form Mn-Mn dimers which would change the $2p$ spectrum. As usual, Lorentzian and Gaussian broadenings and an integrated background have been applied to the theoretical spectrum. Figure 4 shows the best fit reached for $\Delta = 1$ eV, $U = 3$ eV, and $T = 1.2$ eV. For comparison to the case of $c(2\times2)$ Mn/Cu(100) we have repeated the calculation for the $MnCu_8$ cluster in the geometry described in Ref. 8 with the present model, i.e., including multiplet effects. We obtain $\Delta = 1.5$ eV, $U = 3$ eV, and $T = 1.0$ eV for the Cu-based system and an agreement with experiment substantially improved with respect to Ref. 8—almost perfect matching between model and experiment is now reached in Fig. 4. The inclusion of multiplet splittings leads to slightly altered parameters[23] like a reduction of Q (or U) ($\Delta = 0$ eV, $U = 4$ eV, and $T = 0.7$ eV were obtained in Ref. 8). Similarly, inclusion of multiplets has a comparatively strong effect on Δ for the d^5 configuration.[20] Comparison of the two systems of Fig. 4 confirms the expectation that Δ and T, but not U, vary slightly with the chemical environment (Ni and Cu, respectively) of the Mn atom. The small but finite values for the charge-transfer energy Δ are realistic in view of the range obtained for three-dimensional Mn compounds (from $\Delta = 6.5$ eV for MnO to 1.5 eV for MnTe, Ref. 20). The present analysis corroborates $\Delta < U$, which means that in Mn $2p$ photoemission spectra the main peak at lower binding energy is rather dominated by $\underline{c}d^6\underline{L}$ and the satellite at higher binding energy by $\underline{c}d^5$ configurations. From $\Delta < U$ also results that $c(2\times2)$ Mn/Ni(110) and $c(2\times2)$ Mn/Cu(100) can be characterized as charge-transfer compounds, where in practice metallic conductivity of the systems will be provided by the Ni and Cu substrates.

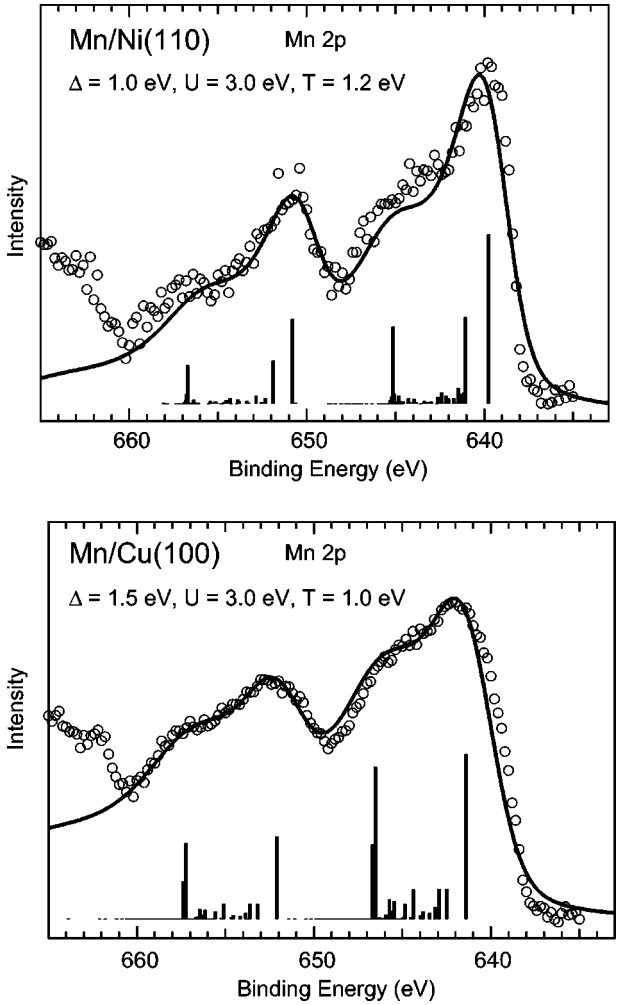

FIG. 4. Configuration-interaction cluster-model theory for $c(2\times2)$ Mn/Ni(110) compared to the measured spectrum of 0.35 ML (top). The case of the well-characterized surface alloy 0.5 ML $c(2\times2)$ Mn/Cu(100) is shown for comparison (bottom).

V. CONCLUSION

It is concluded that geometrical and electronic structure of 0.5 ML Mn on Ni(110) can consistently be described by configuration-interaction theory on a local $MnNi_7$ cluster. It is demonstrated in this way that electronic properties can be used to conclude to some extent on the local geometrical structure of a metal-on-metal adsorbate system. The cluster-model analysis corroborates the view that the local structural arrangement leads to a strong electron correlation effect on the Mn, and together with our LEED study this indicates that an ordered surface alloy $c(2\times2)$ Mn/Ni(110) has been identified in this work.

ACKNOWLEDGMENTS

We thank A. Harasawa for help with the experimental setup. O.R. was supported by the Japan Society for the Promotion of Science and by Alexander von Humboldt-Stiftung and thanks Professor A. Kakizaki for hospitality at Institute for Solid State Physics-SRL.

*Present address: BESSY, Albert-Einstein-Str. 15, D-12489 Berlin, Germany. Electronic address: rader@bessy.de

†Also at Department of Complexity Science and Engineering.

[1] M. Wuttig, Y. Gauthier, and S. Blügel, Phys. Rev. Lett. **70**, 3619 (1993).

[2] See also the review articles by S. Blügel, Appl. Phys. A: Mater. Sci. Process. **63**, 595 (1996); M. Wuttig and B. Feldmann, Surf. Rev. Lett. **3**, 1473 (1996).

[3] M. Wuttig, T. Flores, and C.C. Knight, Phys. Rev. B **48**, 12 082 (1993).

[4] M. Wuttig, C.C. Knight, T. Flores, and Y. Gauthier, Surf. Sci. **292**, 189 (1993); M. Wuttig, B. Feldmann, and T. Flores, *ibid.* **331–333**, 659 (1995).

[5] W.L. O'Brien, J. Zhang, and B.P. Tonner, J. Phys.: Condens. Matter **5**, L515 (1993); W.L. O'Brien and B.P. Tonner, Phys. Rev. B **51**, 617 (1995).

[6] O. Rader, W. Gudat, C. Carbone, E. Vescovo, S. Blügel, R. Kläsges, W. Eberhardt, M. Wuttig, J. Redinger, and F.J. Himpsel, Phys. Rev. B **55**, 5404 (1997).

[7] D. Schmitz, O. Rader, C. Carbone, and W. Eberhardt, Phys. Rev. B **54**, 15 352 (1996).

[8] O. Rader, E. Vescovo, M. Wuttig, D.D. Sarma, S. Blügel, F.J. Himpsel, A. Kimura, K.S. An, T. Mizokawa, A. Fujimori, and C. Carbone, Europhys. Lett. **39**, 429 (1997).

[9] Ch. Ross, B. Schirmer, M. Wuttig, Y. Gauthier, G. Bihlmayer, and S. Blügel, Phys. Rev. B **57**, 2607 (1998).

[10] P. Schieffer, M.C. Hanf, C. Krembel, and G. Gewinner, Surf. Sci. **446**, 175 (2000).

[11] W.L. O'Brien and B.P. Tonner, Phys. Rev. B **50**, 2963 (1994).

[12] B.C. Choi, P.J. Bode, and J.A.C. Bland, Phys. Rev. B **59**, 7029 (1999).

[13] T.G. Walker and H. Hopster, Phys. Rev. B **48**, 3563 (1993).

[14] O. Rader, C. Pampuch, W. Gudat, A. Dallmeyer, C. Carbone, and W. Eberhardt, Europhys. Lett. **46**, 231 (1999).

[15] F. Nouvertne, U. May, A. Rampe, M. Gruyters, U. Korte, R. Berndt, and G. Güntherodt, Surf. Sci. **436**, L653 (1999).

[16] W. Eberhardt and E.W. Plummer, Phys. Rev. B **21**, 3245 (1980); N. Mårtensson, R. Nyholm, and B. Johansson, *ibid.* **30**, 2245 (1984).

[17] Y. Gauthier, M. Poensgen, and M. Wuttig, Surf. Sci. **303**, 36 (1994).

[18] C.R. Brundle and J. Broughton, in *The Chemical Physics of Solid Surfaces and Heterogenous Catalysis*, edited by D.A. King and D.P. Woodruff (Elsevier, New York, 1985).

[19] *Handbook on X-ray Photoelectron Spectroscopy*, edited by G.E. Muilenberg (Perkin-Elmer, Eden Prairie, Minnesota, 1979).

[20] For a review see M. Imada, A. Fujimori, and Y. Tokura, Rev. Mod. Phys. **70**, 1039 (1998).

[21] G. van der Laan, C. Westra, C. Haas, and G.A. Sawatzky, Phys. Rev. B **23**, 4369 (1981).

[22] J. Zaanen, C. Westra, and G.A. Sawatzky, Phys. Rev. B **33**, 8060 (1986).

[23] K. Okada and A. Kotani, J. Phys. Soc. Jpn. **60**, 772 (1991); **61**, 4619 (1992).

[24] A.E. Bocquet, T. Mizokawa, T. Saitoh, H. Namatame, and A. Fujimori, Phys. Rev. B **46**, 3771 (1992); A.E. Bocquet, T. Mizokawa, A. Fujimori, M. Matoba, and S. Anzai, *ibid.* **52**, 13 838 (1995).

[25] A.E. Bocquet and A. Fujimori, J. Electron Spectrosc. Relat. Phenom. **82**, 87 (1996).

[26] W. A. Harrison, *Electronic Structure and the Properties of Solids* (Dover, New York, 1989).